Challenge Journal of Structural Mechanics

Research Article

Robustness evaluation of optimum tuned liquid dampers for uncertain variable loading of structures

Ayla Ocak [a], Gebrail Bekdaş [a], Sinan Melih Nigdeli [a,*]

[a] *Department of Civil Enginering, İstanbul University-Cerrahpaşa, 34320 İstanbul, Turkey*

ABSTRACT

This study focuses on the performance analysis of optimum tuned liquid dampers (TLDs) under the different live loads of three different structure models, designed as both single and multi-story, under earthquake excitations. For this purpose, single, ten, and forty story structure models have been created and tuned liquid damping devices that contain liquids of different densities and viscosities such as acetone, mercury, and seawater are placed on the structure. For the analysis conducted under earthquake excitations, optimum damping device parameters were previously obtained with the Adaptive Harmony Search Algorithm (AHS), and minimizing the movement of the structure was aimed. The effect of the damping device on the control performance was investigated under increasing and decreasing live loads for the uncertain mass of the structure because of variable actions. When the results are examined, it has been determined that the increase in the story number of the structure will less affect the displacement reduction performance of TLDs for the structure under uncertain variable loading.

ARTICLE INFO

Article history:
Received 28 March 2022
Revised 1 May 2022
Accepted 20 May 2022

Keywords:
Tuned liquid damper
Structural control
Optimization
Adaptive harmony search

1. Introduction

Tuned liquid dampers (TLD) are passive control systems that dampen the movement by utilizing the spring stiffness and the sloshing energy of a liquid mass. Similar to other passive control systems, it provides control with the help of the main mass it contains. TLDs are designed according to the selected mass ratio considering the structure mass. However, apart from the mass of the initially accepted structure, the effect of live loads affecting the movement of the structure should be investigated. In structures, the off-tuning of the live load has been investigated for situations such as vibration tests and the addition of a mass damper. Setareh et al. (2006) investigated pendulum-type mass dampers and the optimum values were tested for possible mass change in the controlled floor system. Xing et al. (2014) proposed a tuned mass damper type counterweight for cable-stayed bridges under wind excitation to reduce the live-load amount. The increase in the damping of live loads in suspension bridges due to the mass damper-like motion caused by the presence of vehicles has been investigated in various studies (Wibowo et al. 2014; Shaban et al. 2015). In their study, Venanzi and Materazzi (2013) investigated the effect of uncertain mass distribution on floors in hybrid control of high-rise buildings under the influence of wind loads and conducted a hybrid control design that is resistant to uncertainties in load distribution. In the design of both single and multi-story structures, situations such as the increase in the number of visitors depending on the purpose of use of the structure make it necessary to investigate the live load situation.

TLDs are also known as liquid mass-containing types of tuned mass dampers (TMDs). Due to the presence of a liquid mass in it, the period of the sloshing liquid and its stable mass are both considered in the design. Appropriate selection of the characteristic properties of liquids facilitates control. Properties such as the density and kinematic viscosity of the TLD liquid have been observed in studies that modified TLD derivatives in which various mixtures, balls, and mixtures are used together to have a

* *Corresponding author*. Tel.: +90-212-473-7070 ; Fax: +90-212-473-7176 ; E-mail address: melihnig@iuc.edu.tr (S. M. Nigdeli)
ISSN: 2149-8024 / DOI: https://doi.org/10.20528/cjsmec.2022.03.001

churning and damping effect (Hitchcock et al. 1997; Tanveer et al. 2020; Shah et al. 2022). It is known that the optimization of these parameters with various optimization methods can increase control efficiency. Generally, parametric optimization has been performed for TLDs since the 90s (Gao et al. 1997; Xue et al. 2000; Taflanidis et al. 2005; Shum 2009; Debbarma et al. 2010; Mehrikan and Altay 2020; Ocak et al. 2022).

In this study, the optimum TLD parameters obtained from the Ocak et al. (2022) using different liquids with single-story, ten-story, and 40-story structure models were investigated for different structure mass situations on the same structure models. The optimum parameters for a constant mass of the structure are taken in all cases and possible changes in live loads were considered for TLD performance. All comparisons of the control system were done with the results of uncontrolled structure with the changing masses. As known, the most effective index in the optimum tuning of mass dampers is the critical natural frequency of the structure, and the mass change will change the frequency of the structure and the optimum TLD system may get out of tune.

In their study, Ocak et al. (2022) investigated the effects of viscosity and density on the selection of the optimum TLD liquid of different liquids and different structure models. In the results obtained for a single-story structure, it was determined that less dense liquid with lower viscosity is optimum, as the number of stories increases, viscosity, and density are desired to be higher, and in heavy structures such as 40 floors, viscosity loses its importance and density comes to the fore (Ocak et al. 2022). In this study, considering the work of Ocak et al. (2022), acetone and mercury liquids, which are the optimum TLD liquids obtained in the single-story and forty-story structure model, were used. In the ten-story structure model they used in the study, propanol and seawater liquids were very close in percentage, and small fractional differences were found. In the study, seawater liquid was preferred for the ten-story structure model, since it would be more cost-effective to obtain seawater.

Critical earthquake analysis was carried out for all cases. The control performance of TLDs has been investigated in case the structure mass changes. FEMA records, which include 22 earthquake records, were excited as an excitation to the structure models via Matlab Simulink (FEMA P-695 2009; Matlab 2018). Analyzes were made using optimum TLD parameters and optimum liquid. The effect of the increase and decrease in the mass of the multi-story structure models on the damper performance has been investigated. Performance analysis was made by increasing or decreasing the structure mass up to 25%. The impact of structure and variable actions on TLD performance has been researched. The results obtained for the multi-story structures were compared with the mass change results obtained in the single-story structure model obtained by Ocak et al. (2022).

2. Design of Tuned Liquid Dampers

2.1. Equations of motion

Tuned liquid dampers dampen the movement of the structure with the mechanical energy arising from the sloshing of the liquid in the tank. The main parameters affecting this energy depend on the damper mass, tank geometry and period, and properties such as damping ratio. It is suggested in the literature that the mass ratio of TLDs can be selected between 1-5%, considering the recommended ratio for mass dampers (Sun et al. 1992; Yu et al. 1999; Vickery et al. 1983; Rana and Soong 1998). In the sloshing model of a cylindrical tank created according to the linear hydrodynamic theory, TLD liquid is divided into two sloshing and non-sloshing liquids (Abramson 1966). It is designed according to the assumption that while the sloshing liquid moves with separate freedom, the inactive liquid moves together with the tank. In Fig. 1, the TLD mechanical model placed on a single-story structure is given.

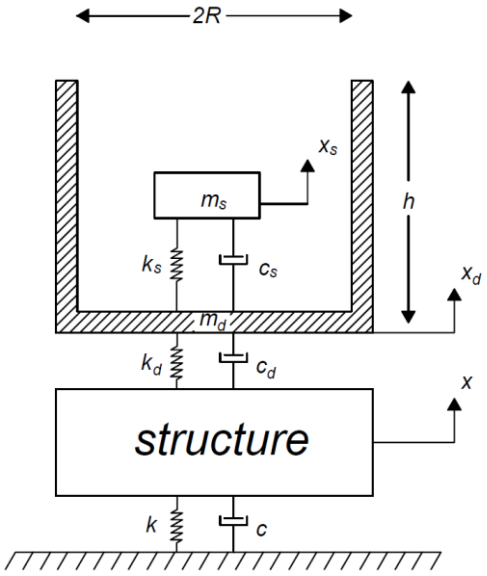

Fig. 1. Cylindrical TLD model placed in a single-story structure (Ocak et al. 2022).

For the calculation of the sloshing liquid mass, the damping ratio parameter (ξmn) with tangential (m) and radial (n) directions, which is expressed as the roots of the Bessel function used in the wave propagation of cylindrical bodies, is used (Sharma et al. 2019). By setting this parameter to the 1st Vibration mode, the sloshing liquid mass equation is created with a coefficient of 1.84, and by using it in the calculation of the lateral forces in the tank, the frequency and stiffness of the sloshing liquid are calculated (Bauer 1964; Rouf 2005; Sharma et al. 2019). The calculation of the sloshing active liquid mass (m_s) in the tank is shown in Eq. (1).

$$m_s = m_{st} \times R \times \frac{\tanh\left(\frac{1.84h}{R}\right)}{2.2h} \quad (1)$$

where m_{st} is the total mass of liquid in the tank, R is the radius of the cylindrical tank and h is the height of the liquid in the tank.

The non-sloshing liquid, which represents the second freedom of the damper, and the mass in which the tank moves together are expressed as m_d. It is obtained by subtracting the mass of sloshing liquid from the total mass of TLD (m_{TLD}). In Eq. (2), the empty mass of the tank and the total mass of the liquid that is not sloshing (m_d) are calculated.

$$m_d = m_{TLD} - m_s \tag{2}$$

The stiffnesses (k_d and k_s) of the damper and the sloshing liquid are shown in Eqs. (3) and (4), respectively, and the damping coefficients (c_d and c_s) are shown in Eqs. (5) and (6), respectively.

The stiffnesses (k_d and k_s) of the damper and the sloshing liquid are shown in Eqs. (3) and (4), respectively, and the damping coefficients (c_d and c_s) are shown in Eqs. (5) and (6), respectively.

$$k_d = m_d \times \left(\frac{2\pi}{T_d}\right)^2 \tag{3}$$

$$k_s = m_{st} \times \frac{g\left\{\tanh\left(\frac{1.84h}{R}\right)\right\}^2}{1.19h} \tag{4}$$

$$c_d = 2 \times \zeta_d \times \sqrt{m_d \times k_d} \tag{5}$$

$$c_s = \zeta_s \times 2\sqrt{m_s k_s} \tag{6}$$

The T_d parameter used in Eq. (3) represents the period of the damper tank. The damping ratio (ζ_d) of the damper is given in Eq. (7). The damping ratio (ζ_s) calculation of the shaking is obtained by experimental studies and calculated as in Eq. (8).

$$\zeta_d = \frac{c_d}{2m_d\sqrt{\frac{k_d}{m_d}}} \tag{7}$$

$$\zeta_s = 4.98 v^{\frac{1}{2}} R^{-\frac{3}{4}} g^{-\frac{1}{4}} \left[1 + \frac{0.318}{\sinh\left(\frac{1.84h}{R}\right)} \frac{1-\frac{h}{R}}{\cosh\left(\frac{1.84h}{R}\right)}\right] \tag{8}$$

The g in the equations denotes the gravitational acceleration and v denotes the kinematic viscosity.

The equation of motion of the system in its simplest form, which includes the information about the sloshing liquid, TLD tank + passive liquid, and structure, is shown in Eq. (9), and the mass, stiffness, and damping coefficient matrices are shown in Eq. (10-12), respectively. Terms such as mass, stiffness, and damping coefficient of the structure are included without indexes in the equations.

$$[M]\{\ddot{X}\} + [C]\{\dot{X}\} + [K]\{X\} = -[M]\{1\}\ddot{X}_g \tag{9}$$

A dot in the equations represents the velocity vector, the double dot represents the acceleration vector. Parameter $\ddot{X}_a$ with double dot specifies ground acceleration. {1} represents a vector of ones.

$$[M] = \begin{bmatrix} m & 0 & 0 \\ 0 & m_d & 0 \\ 0 & 0 & m_s \end{bmatrix} \tag{10}$$

$$[K] = \begin{bmatrix} k + k_d & -k_d & 0 \\ -k_d & k_d + k_s & -k_s \\ 0 & -k_s & k_s \end{bmatrix} \tag{11}$$

$$[C] = \begin{bmatrix} c + c_d & -c_d & 0 \\ -c_d & c_d + c_s & -c_s \\ 0 & -c_s & c_s \end{bmatrix} \tag{12}$$

3. Numerical Examples

In this study, a structure model with three different floors was used. A single-story structure with a weight of 100 tons, a ten-story structure with a weight of 3600 tons, and a forty-story structure with a weight of 39200 tons were designed. The single-story structure model is designed with 3 degrees of freedom (3DOF) taking into account the freedom of the structure, the sloshing liquid, and the TLD tank. Fig. 2 shows a single-story structure model. The period of the single-story structure was chosen as 1 second, and the stiffness and damping coefficients were taken as 3.95 MN/m and 0.06 MNs/m, respectively.

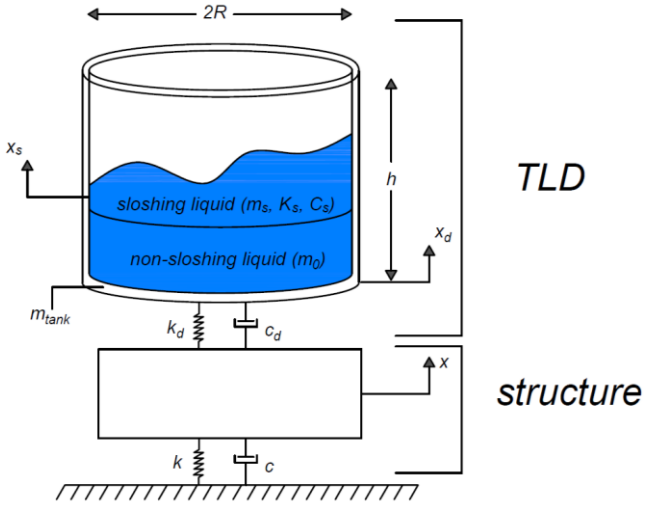

Fig. 2. Cylindrical TLD model placed in a single-story structure.

Twelve degrees of freedom (12DOF) as ten-story structure, ten-story freedom, sloshing liquid freedom, and TLD tank freedom were taken into account, and the structural stiffness and damping coefficient values were taken as 650 MN/m and 6.2 MNs/m, respectively (Singh et al. 2002). For the forty-story structure model, these values were used in the analysis as 2130 MN/m and 42.6 MNs/m on the first floor of the structure and 998 MN/m and 20 MNs/m on the last floor of the structure (Liu et

al. 2008). The multi-story structure model used is shown in Fig. 3. Here, the "*i*" index indicates the floor number, and the "*n*" index indicates the top floor number of the structure.

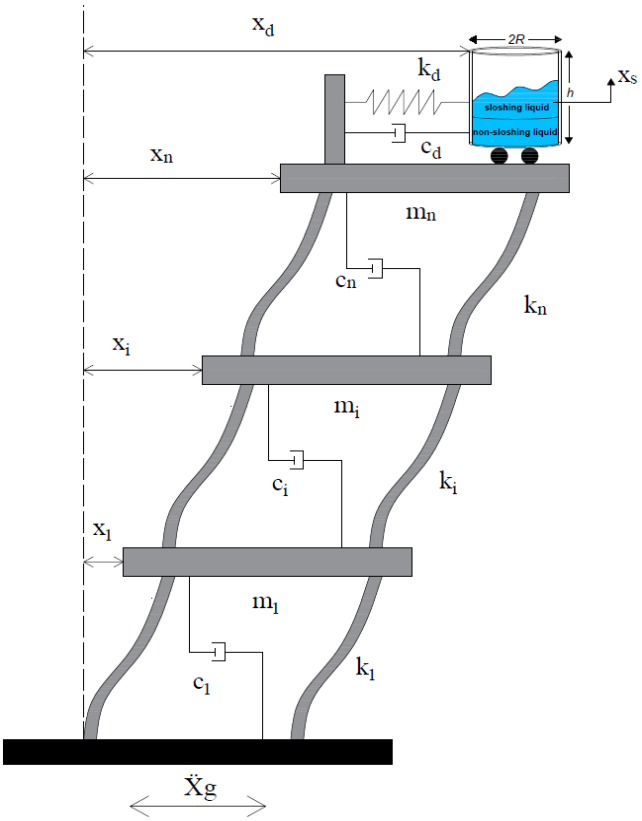

Fig. 3. Cylindrical TLD model placed in a multi-story structure.

TLDs are placed on the models created for the application. FEMA earthquake records consisting of various earthquakes were excited to the structures in Matlab Simulink and optimum results were found in Ocak et al. (2022). The earthquake records are listed in Table 1.

Ocak et al. (2022) determined that among the liquids they used, acetone for a single-story liquid, seawater for a ten-story structure, and mercury for a forty-story structure were the optimum liquids as TLD liquids. These liquid types were used for each structure model in which TLD was placed. The optimum TLD parameters for single-story, ten, and forty-story structure models are shown in Table 2.

As a result of the earthquake analysis, the critical earthquake record for the single-story and ten-story structures was DUZCE/BOL090, CHICHI/CHY101-N for the forty-story structure according to results in Ocak et al. (2022). In the analysis conducted with optimum TLD parameters, the effects of live loads on displacement and total acceleration with ∓25% mass change for selected liquids were investigated. The displacement and total acceleration values obtained under the effect of live loads for critical earthquake recording in a single-story, ten- and forty-story structure are shown in Table 3. In Table 3, the critical earthquake analysis results obtained from the multi-story building models are presented together with the mass change results on the single-story building model in the work of Ocak et al. (2022).

As a result of the critical earthquake analysis, the displacement-time and total acceleration-time graphs obtained at -25% mass decrease for a single-story structure are given in Fig. 4, and the displacement-time and total acceleration-time graphs obtained at +25% mass increase are also shown in Fig. 5.

Table 1. FEMA earthquake records list.

Earthquake Number	Date	Earthquake Name	Component 1	Component 2
1	1994	Northridge	NORTHR/MUL009	NORTHR/MUL279
2	1994	Northridge	NORTHR/LOS000	NORTHR/LA270
3	1999	Duzce, Turkey	DUZCE/BOL0000	DUZCE/BOL090
4	1999	Hector Mine	HECTOR/HEC000	HECTOR/HEC090
5	1979	Imperial Valley	IMPVALL/H-DLT262	IMPVALL/H-DLT352
6	1979	Imperial Valley	IMPVALL/H-E11140	IMPVALL/H-E11230
7	1995	Kobe, Japan	KOBE/NIS000	KOBE/NIS090
8	1995	Kobe, Japan	KOBE/SHI000	KOBE/SHI090
9	1999	Kocaeli, Turkey	KOCAELI/DZC180	KOCAELI/DZC270
10	1999	Kocaeli, Turkey	KOCAELI/ARC000	KOCAELI/ARC090
11	1992	Landers	LANDERS/PLACE270	LANDERS/YER360
12	1992	Landers	LANDERS/CLW-LN	LANDERS/CLW-TR
13	1989	Loma Prieta	LOMAP/CAP000	LOMAP/CAP090
14	1989	Loma Prieta	LOMAP/G03000	LOMAP/G03090
15	1990	Manjil, Iran	MANJIL/ABBAR--L	MANJIL/ABBAR--T
16	1987	Superstition Hills	SUPERST/B-ICC000	SUPERST/B-ICC090
17	1987	Superstition Hills	SUPERST/B-POE270	SUPERST/B-POE360
18	1992	Cape Mendocino	CAPEMEND/RIO270	CAPEMEND/RIO360
19	1999	Chi-Chi, Taiwan	CHICHI/CHY101-E	CHICHI/CHY101-N
20	1999	Chi-Chi, Taiwan	CHICHI/TCU045-E	CHICHI/TCU045-N
21	1971	San Fernando	SFERN/PEL090	SFERN/PEL180
22	1976	Friuli, Italy	FRIULI/A-TMZ000	FRIULI/A-TMZ270

Table 2. Optimum TLD parameters for single, ten, and forty story structure models (Ocak et al. 2022).

Variables	Single story structure	10-storey structure	40-storey structure
	Acetone	Seawater	Mercury
T_d (s)	0.9454	0.9962	3.5626
ζ_d	0.0810	0.1841	0.2270
R (m)	0.5418	1.1087	4.1312
h (m)	2.2884	0.7556	2.3684

Table 3. Displacement and total acceleration values obtained by the effect of live load in the critical earthquake record for single-story, ten and forty-story structure models.

Structure mass increase/decrease percentage	Single-story Structure with TLD-Acetone		10-story Structure with TLD-Seawater		40-story Structure with TLD-Mercury	
	Displacement (m)	Total Acceleration (m/s²)	Displacement (m)	Total Acceleration (m/s²)	Displacement (m)	Total Acceleration (m/s²)
-25%	0.2016451	10.5720449	0.2559605	15.1735650	1.0073726	5.0971812
-20%	0.2121752	10.4000571	0.2696159	15.2311032	1.0755072	4.8098033
-15%	0.2208049	10.1468190	0.2806673	15.1687362	1.1373364	5.0038573
-10%	0.2274021	9.8344712	0.2890280	14.9887245	1.1940244	5.2571767
-5%	0.2319002	9.4777271	0.2944632	14.7042480	1.2967174	5.2711654
0%	0.2343740	9.0757597	0.2971696	14.3177283	1.4018155	5.1254171
+5%	0.2386721	8.6500651	0.3031982	13.8256268	1.5088005	4.9823147
+10%	0.2446614	8.4727027	0.3104425	13.2362306	1.6210147	4.9097424
+15%	0.2493544	8.2673290	0.3160396	12.5673918	1.7406651	4.8223275
+20%	0.2526405	8.0375150	0.3198721	11.8227165	1.8659784	4.6367295
+25%	0.2544804	7.7830968	0.3219217	11.4095860	1.9924649	4.8080075

As a result of the critical earthquake analysis, the displacement-time and total acceleration-time graphs obtained at -25% mass decrease for the ten-story structure are shown in Fig. 6, and the displacement-time and total acceleration-time graphs obtained at +25% mass increase are also given in Fig. 7.

As a result of the critical earthquake analysis, the displacement-time and total acceleration-time graphs obtained at -25% mass decrease for the forty-story structure are reported in Fig. 8, and the displacement-time and total acceleration-time graphs obtained at +25% mass increase are plotted in Fig. 9.

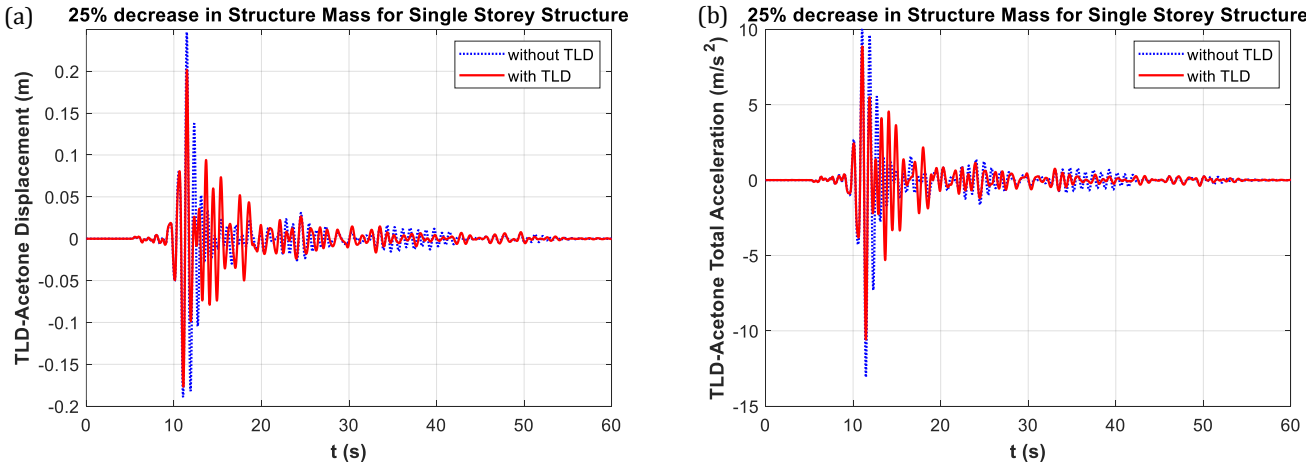

Fig. 4. Graphs obtained from the critical earthquake analysis for a single-story structure at a 25% mass decrease: (a) Displacement-time; (b) Total acceleration-time.

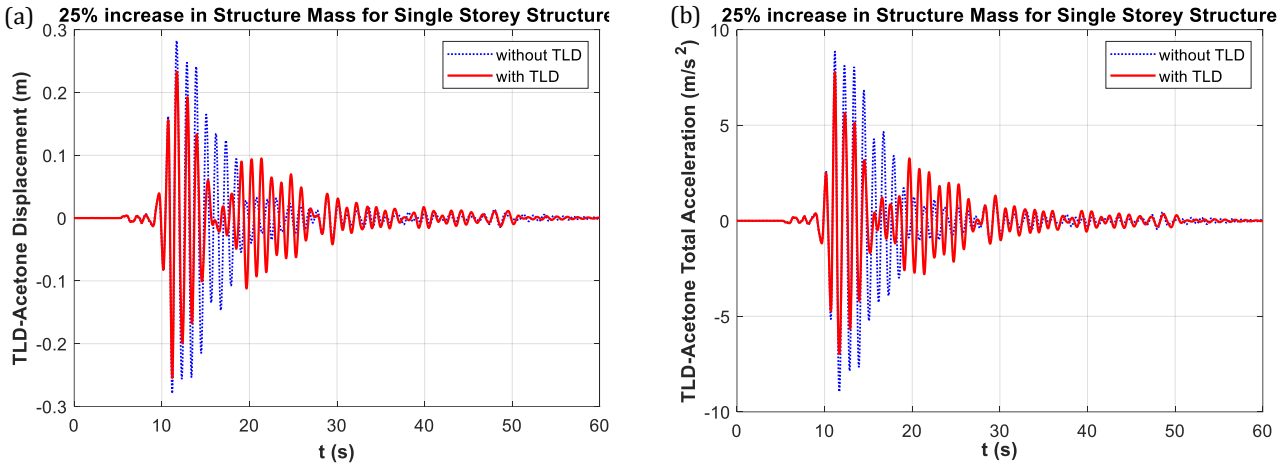

Fig. 5. Graphs obtained from the critical earthquake analysis for a single-story structure at a 25% mass increase: (a) Displacement-time; (b) Total acceleration time.

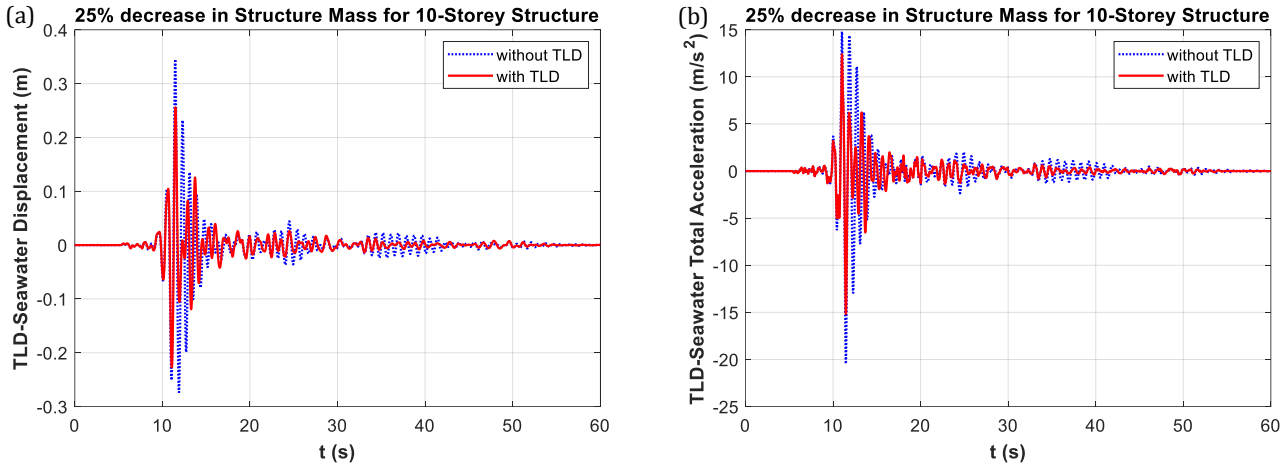

Fig. 6. Graphs obtained from the critical earthquake analysis for a 10-story structure at a 25% mass decrease: (a) Displacement-time; (b) Total acceleration-time.

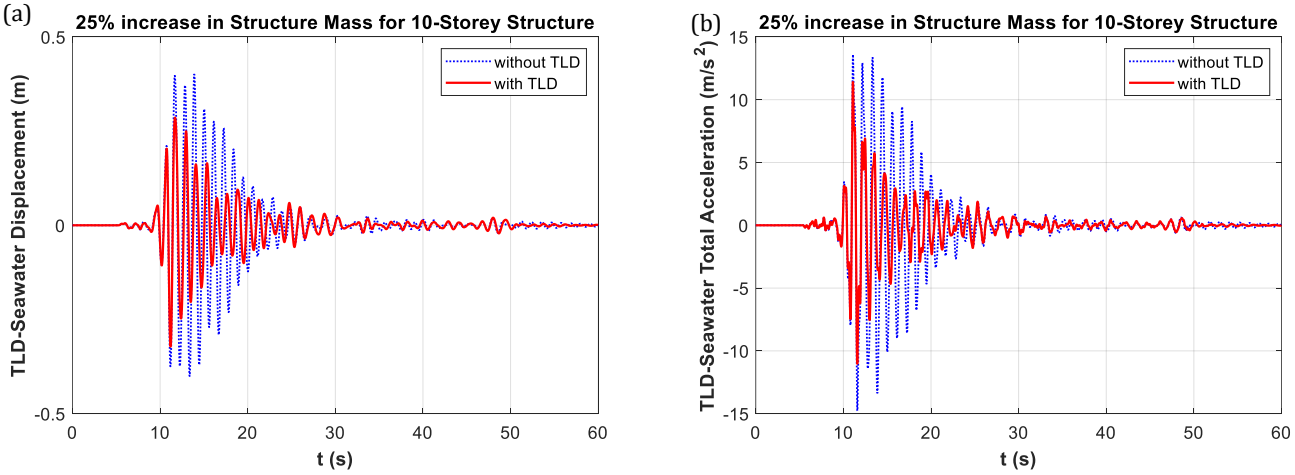

Fig. 7. Graphs obtained from the critical earthquake analysis for a 10-story structure at a 25% mass increase: (a) Displacement-time; (b) Total acceleration-time.

(b)

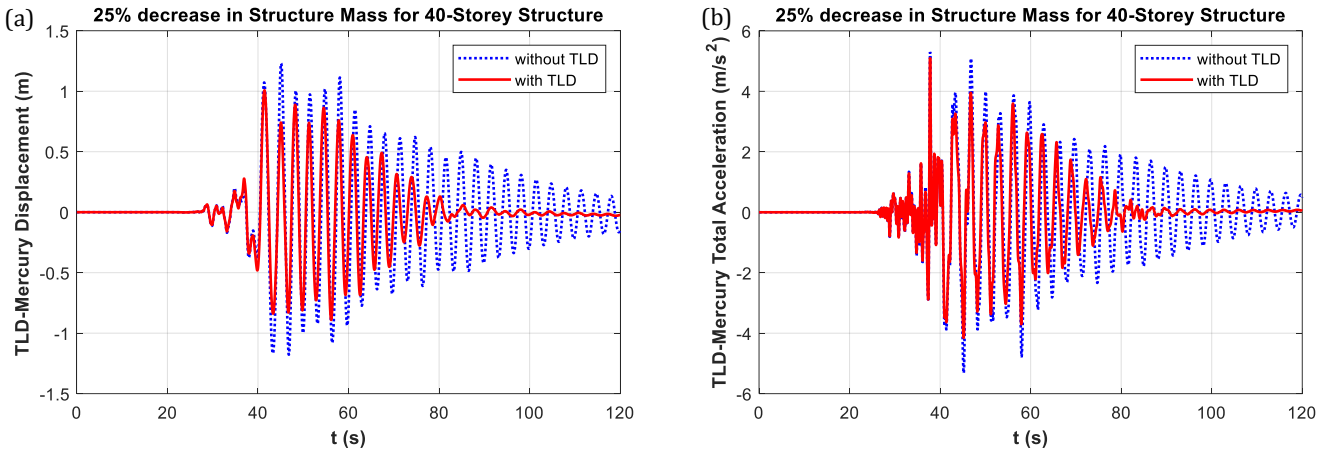

Fig. 8. Graphs obtained from the critical earthquake analysis for a 40-story structure at a 25% mass decrease: (a) Displacement-time; (b) Total acceleration-time.

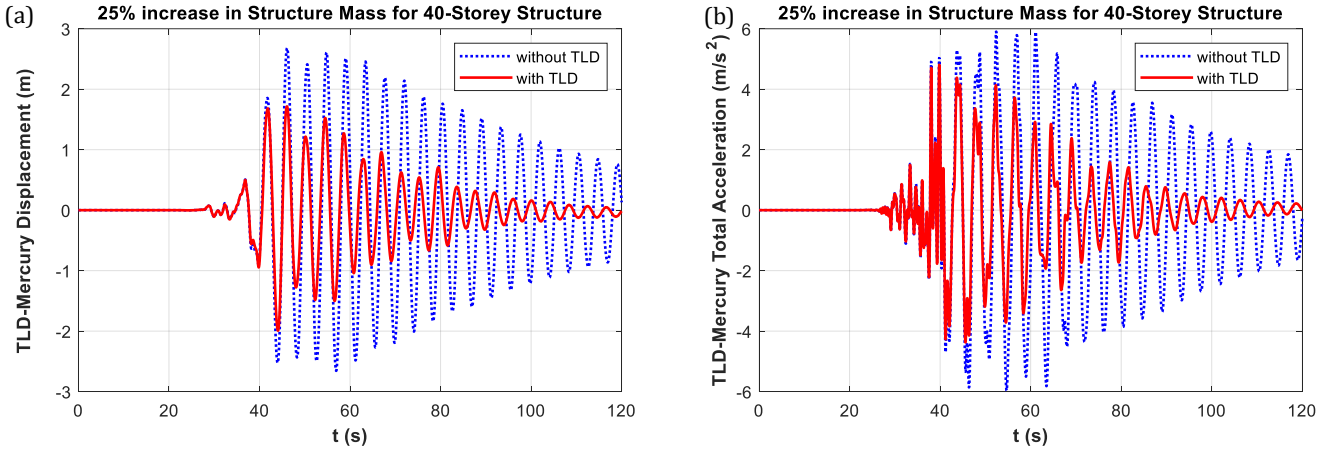

Fig. 9. Graphs obtained from the critical earthquake analysis for a 40-story structure at a 25% mass increase: (a) Displacement-time; (b) Total acceleration-time.

4. Discussion

In this study, analyzes were made under earthquake excitations to observe the effect of live load on single-story ten-story, and forty-story structure models using optimum TLD parameters and optimum liquid types. Critical earthquake record was determined in FEMA earthquake records for each structure model and TLD was analyzed under these earthquake excitations. Results evaluated for up to 25% increase and decrease of structure mass. In Table 4, displacement and total acceleration decrease percentages are given.

When Table 4 is examined, in the analyzes made for a single-story structure, the maximum displacement reduction performance was observed at a rate of 18.79%, and the minimum displacement reduction performance was observed at a rate of 9.91% when the structure mass was decreased by 15%. While the displacement reduction quality of TLDs shows an increasing graph up to the case where the structure mass is reduced by 15% for the example single-story structure model, the increased load state after this value is adversely affected. In the 100 tons model, the mass change in the structure with the effect of live load from 85 tons to 125 tons reduced the displacement reduction ability of TLD performance by approximately 9%. Although the total acceleration reduction performance did not lose as fast as the displacement with the increase in mass, each increase after the 5% increase in the mass also negatively affected the total acceleration. When comparing the optimum overall deceleration performance with the worst TLD performance, a performance loss of 7.5% is observed. For single-story structures, it can be said that the increase in mass significantly affects both the displacement and the overall acceleration reduction performance of TLDs.

In the ten-story structure analyzes, the maximum displacement reduction percentage of TLD was 27.55% and the minimum displacement reduction percentage was 19.67%. From the moment the mass started to be increased, the displacement reduction effect started to decrease, while each other increased mass percentage from the case where the mass was reduced by 10% also negatively affected the total acceleration. There is a performance loss for a displacement of about 8% and a reduction of total acceleration of 4%. It is seen that the live load effect does not significantly affect the TLD performance in terms of acceleration reduction of ten-story structures, but there is still a loss in displacement that should be noted.

Table 4. Displacement and total acceleration reduction percentages obtained by the effect of live load in the critical earthquake record for single-story, 10-storey, and 40-story structure models.

Structure mass increase/decrease percentage	Single-story Structure with TLD-Acetone		10-story Structure with TLD-Seawater		40-story Structure with TLD-Mercury	
	Displacement (m)	Total Acceleration (m/s²)	Displacement (m)	Total Acceleration (m/s²)	Displacement (m)	Total Acceleration (m/s²)
-25%	18.27	19.17	25.88	25.85	18.02	4.17
-20%	18.71	19.80	26.90	26.61	23.08	16.42
-15%	18.79	20.15	27.40	26.79	26.41	18.77
-10%	18.71	20.32	27.53	26.61	28.73	17.70
-5%	18.57	20.38	27.55	26.21	27.92	17.10
0%	18.43	20.44	27.54	25.75	27.28	16.98
+5%	17.13	20.52	26.19	25.44	26.96	17.32
+10%	14.88	18.23	24.17	25.29	26.79	17.93
+15%	12.86	16.16	22.25	25.26	26.55	18.38
+20%	11.17	14.40	20.78	25.31	26.15	18.68
+25%	9.91	13.02	19.67	22.70	25.66	19.36

In the critical earthquake analysis of the forty-story building model, each mass increase since the 10% reduction in the mass weakened the displacement reduction effect of the TLD. The maximum displacement reduction percentage, which was 28.73% for different structure mass situations given in Table 4, decreased to 25.66% as the mass increased. TLD performance loss was observed in terms of displacement reduction of approximately 3%. In the forty-story structure model, the increase in structure mass increased the overall acceleration performance by about 15%, in contrast to the decrease in displacement.

Above, the effect of change in structure mass on TLD displacement and total acceleration reductions is described. By converting TLD performance from the structure mass change to a percentage, it becomes easier to understand the effect of mass on performance. The optimum displacement reduction value in a single-story structure was observed at 15% mass reduction. From this to the case where the mass is increased by up to 25%, the TLD displacement reduction performance is reduced by approximately 47% and the total acceleration performance by approximately 37%. While the mass reduction in the ten-story structure affected the displacement reduction performance by approximately 6%, the 25% mass increase decreased the displacement and total acceleration reduction performance of the TLD by approximately 29% and 12%. In the forty-story structure example, the displacement reduction performance of the TLD decreased by approximately 10.7%, from 10% mass reduction where the optimum displacement reduction percentage was observed, to 25% mass increase. The effect of reducing the total acceleration showed a regular increase from 25% mass reduction to 25% mass increase. The overall deceleration performance of the TLD increased by approximately 8.6% for the final state of the increased mass from the state where the optimum displacement reduction percentage was shown.

5. Conclusions

According to the results, the following information is obtained.

- It is seen that the increase in mass of the structure creates a performance loss of approximately 47% for displacement and approximately 37% for total acceleration. It is understood that considering the live load effect in the design of a single-story structure is of great importance for the safety of the design.
- Although the live load creates less performance loss for a ten-story structure model than for a single-story structure, it is seen that the damper's displacement reduction performance affects 29% seriously and it should be taken into account in the designs.
- While decreasing the displacement reduction percentage in a forty-story structure, it is seen that the increase in mass has a positive effect on the damper in terms of reducing the total acceleration. There is a lower performance loss in terms of displacement compared to a single-story and ten-story structure. Based on this, it is understood that as the number of floors increases, the mass change decreases the effect of the damper on the displacement reduction performance.
- For the 40-story structure with TLD-Mercury, the mass change is not so effective on the change of the total acceleration values.

In light of all the information, it can be said that live loads can seriously affect the damper performance, especially in structures with a small number of floors.

Acknowledgements

None declared.

Funding

The authors received no financial support for the research, authorship, and/or publication of this manuscript.

Conflict of Interest

The authors declared no potential conflicts of interest with respect to the research, authorship, and/or publication of this manuscript.

References

Abramson HN (1966). The dynamic behavior of liquids in moving containers. *NASA Special Publication*, SP-106.

Bauer HF (1964). Tables and graphs of zeros of cross-product Bessel functions. *Mathematics of Computation*, 18(85), 128.

Debbarma R, Chakraborty S, Ghosh SK (2010). Optimum design of tuned liquid column dampers under stochastic earthquake load considering uncertain bounded system parameters. *International journal of mechanical sciences,* 52(10), 1385-1393.

FEMA P-695 (2009). Quantification of Structure Seismic Performance Factors. Washington.

Gao H, Kwok KCS, Samali B (1997). Optimization of tuned liquid column dampers. *Engineering Structures,* 19(6), 476-486.

Hitchcock PA, Kwok KCS, Watkins RD, Samali B (1997). Characteristics of liquid column vibration absorbers (LCVA)–I. *Engineering Structures*, 19(2), 126-134.

Liu, M. Y., Chiang, W. L., Hwang, J. H., & Chu, C. R. (2008). Wind-induced vibration of a high-rise building with tuned mass damper including soil-structure interaction. *Journal of Wind Engineering and Industrial Aerodynamics*, 96(6-7), 1092-1102.

Matlab R2018a (2018). The MathWorks, Natick, MA.

Mehrkian B, Altay O (2020). Mathematical modeling and optimization scheme for omnidirectional tuned liquid column dampers. *Journal of Sound and Vibration,* 484, 115523.

Ocak A, Bekdaş G, Nigdeli SM, Kim S, Geem ZW (2022). Optimization of tuned liquid damper including different liquids for lateral displacement control of single and multi-story structures. *Buildings*, 12(3), 377.

Rana R and Soong TT (1998). Parametric study and simplified design of tuned mass dampers. *Engineering Sructures,* 20(3), 193-204.

Rouf AI (2005). Liquid Sloshing Dynamics: Theory and Applications, Cambridge University Press, ISBN: 0-521-83885-1.

Setareh M, Ritchey JK, Baxter AJ, Murray TM (2006). Pendulum-tuned mass dampers for floor vibration control. *Journal of Performance of Constructed Facilities*, 20(1), 64-73.

Shaban N, Caner A, Yakut A, Askan A, Karimzadeh Naghshineh A, Domanic A, Can G (2015). Vehicle effects on seismic response of a simple-span bridge during shake tests. *Earthquake Engineering & Structural Dynamics*, 44(6), 889-905.

Shah MU, Usman M, Farooq SH, Kim IH (2022). Effect of tuned spring on vibration control performance of modified liquid column ball damper. *Applied Sciences*, 12(1), 318.

Sharma V, Arun CO, Krishna IP (2019). Development and validation of a simple two degree of freedom model for predicting maximum fundamental sloshing mode wave height in a cylindrical tank. *Journal of Sound and Vibration*, 461, 114906.

Shum KM (2009). Closed-form optimal solution of a tuned liquid column damper for suppressing harmonic vibration of structures. *Engineering Structures*, 31(1), 84-92.

Singh MP, Singh S, Moreschi LM (2002). Tuned mass dampers for response control of torsional buildings. *Earthquake Engineering & Structural Dynamics*, 31(4), 749-769.

Sun LM, Fujino Y, Pacheco BM, Chaiseri P (1992). Modeling of tuned liquid damper (TLD). *Journal of Wind Engineering and Industrial Aerodynamics,* 43(1-3), 1883-1894.

Taflanidis AA, Angelides DC, Manos GC (2005). Optimal design and performance of liquid column mass dampers for rotational vibration control of structures under white noise excitation. *Engineering Structures,* 27(4), 524-534.

Tanveer M, Usman M, Khan IU, Farooq SH, Hanif A (2020). Material optimization of tuned liquid column ball damper (TLCBD) for the vibration control of multi-story structures using various liquid and ball densities. *Journal of Structure Engineering*, 32, 101742.

Venanzi I, Materazzi AL (2013). Robust optimization of a hybrid control system for wind-exposed tall buildings with uncertain mass distribution. *Smart Structures and Systems*, 12(6), 641-659.

Vickery BJ, Isyumov N, Davenport AG (1983). The role of damping, mass, and acceleration *Journal of Wind Engineering and Industrial Aerodynamics*, 11(1-3), 285-294.

Wibowo H, Sanford DM, Buckle IG, Sanders DH (2014). Preliminary parametric study of the effects of live load on seismic response of highway bridges. In *Proceedings of the 10th US National Conference on Earthquake Engineering. Earthquake Engineering Research Institute*.

Xing C, Wang H, Li A, Xu Y (2014). Study on wind-induced vibration control of a long-span cable-stayed bridge using TMD-type counterweight. *Journal of Bridge Engineering*, 19(1), 141-148.

Xue SD, Ko JM, Xu YL (2000). Optimum parameters of tuned liquid column damper for suppressing pitching vibration of an undamped structure. *Journal of Sound and Vibration*, 235(4), 639-653.

Yu JK, Wakahara T, Reed DA (1999). A non-linear numerical model of the tuned liquid damper. *Earthquake Engineering & Structural Dynamics,* 28(6), 671-686.